内蒙古阿巴嘎旗阿德拉嘎碱长花岗岩锆石 LA-ICP-MS U-Pb 年龄、地球化学特征及构造意义

赵泽南,魏民,杨建坤,倪克庆,张建珍,申晋青,刘腾飞,葛斌
河北省区域地质调查院,河北廊坊, 065000

内容提要: 阿巴嘎旗阿德拉嘎碱长花岗岩位于贺根山蛇绿岩带北侧。为了确定该碱长花岗岩体的岩石成因类型,探讨其构造环境,对该岩体进行了野外地质、岩石学、地球化学和 LA-ICP-MS 锆石 U-Pb 年代学研究。锆石 LA-ICP-MS U-Pb 测年表明,阿德拉嘎碱长花岗岩体的侵位年龄为 310.7±2.6Ma,形成时代为晚石炭世。岩石地球化学研究表明,阿德拉嘎碱长花岗岩具有较高的 SiO_2、Na_2O+K_2O 含量和较高的 Ga/Al、$(Na_2O+K_2O)/CaO$ 值,相对贫 CaO、MgO、Sr、Ba、Eu、Ti 和 P。稀土元素总量较低,轻重稀土分馏不明显,稀土配分曲线呈海鸥性,负铕异常明显(δEu=0.15~0.37)。岩石学和岩石地球化学特征表明,该碱长花岗岩为 A 型花岗岩,形成于弧后伸展构造环境,为晚石炭世古亚洲洋向西伯利亚俯冲作用的产物。

关键词:碱长花岗岩;A 型花岗岩;锆石 U-Pb 定年;晚石炭世;弧后伸展环境;内蒙古阿巴嘎旗

A 型花岗岩概念最早由 Loiselle 和 Wones (1979) 提出,原始定义为碱性(alkaline)、贫水(anhydrous)和非造山(anorogenic)的花岗岩。A 型花岗岩概念提出后,由于其特殊的成因、产出构造背景和重要的地球动力学意义,引起广大地质工作者的关注(Whalen et al. ,1987;Sylvester,1989;Bonin,1990;Eby,1990,1992;Whalen et al. ,1996;King et al. ,1997;Bonin,2007)。Whalen et al. (1987) 认为 A 型花岗岩具有高 Ga/Al 等地球化学特点,并建立了相应的 A 型花岗岩判别图解。Eby(1992)将 A 型花岗岩划分为 A_1 和 A_2 两个亚类,A_1 亚类与洋岛玄武岩(OIB)有一定相似性,产于板内构造环境,A_2 亚类与岛弧玄武岩有一定相似性,产于后碰撞构造环境。Bonin(2007)对 A 型花岗岩研究进行了总结,并将 A 型花岗岩定义扩大为碱性(alkaline)、贫水(anhydrous)、非造山(anorogenic)、铝质(aluminous)及模棱两可的(Ambiguous),认为 A 型花岗岩可以形成于从陆内到大陆边缘的各种动力学背景或构造环境。

中亚造山带(CAOB)是位于西伯利亚板块与塔里木—华北板块之间的巨型复合造山带,其东段延伸至我国内蒙古及东北地区,被称为兴蒙造山带(图 1)。前人在造山带与古亚洲洋演化方面取得较大成果(Sengor et al. ,1993;Dobretsov et al. ,1995;Xiao Wenjiao et al. ,2003;张磊等,2013;Zhu Mingshuai et al. ,2014;邓晋福等,2015;刘锐等,2016;田树刚等,2016;李钢柱等,2017;王金芳等,2017,2019,2020,2021;李英杰等,2018;王树庆等,2018,2020;张晓飞等,2018a,b,2019;程杨等,2019,2020;范玉须等,2019,2020;李锦轶等,2019a,b;董培培等,2021;李英雷等,2021;张夏炜等,2021;金松等,2022;杨晓平等,2022)。古亚洲洋于寒武纪之前打开(Tang Kedong,1990;Zhu Mingshuai et al. ,2014)。寒武纪—志留纪古亚洲洋开始向南北两侧发生双向俯冲(Xiao Wenjiao et al. ,2003),俯冲持续到石炭纪—早中二叠世(Xiao Wenjiao et al. ,2003;张磊等,2013;李英杰等,2018;王树庆等,2018;张晓飞等,2018a,b,2019;王金芳等,2017,2019,2020,2021;程杨等,2019,2020;范玉须等,2019,2020;董培培等,2021;李英雷等,2021;张夏炜等,2021;金松等,2022;杨晓平等,2022)。古亚洲洋东部最终在晚二叠世末—早三叠世初关闭(Sengor et al. ,1993;Xiao Wenjiao et al. ,2003;邓晋福等,2015;刘锐等,2016;田树刚等,2016)。最近,吕洪波等(2018)在

注:本文为中国地质调查局"内蒙古翁根温多尔等八幅 1∶5 万矿产调查项目"(编号:1212011220451)的成果。
收稿日期:2022-04-13;改回日期:2022-10-09;网络首发:2022-10-20;责任编辑:章雨旭。Doi:10.16509/j.georeview.2022.10.065
作者简介:赵泽南,男,1985 年生,工程师,硕士,主要从事区域地质和矿产地质调查;Email:zhaozenan1985@126.com。

狼山发现白垩纪蛇绿混杂岩,认为古亚洲洋与华北克拉通是在白垩纪沿儿狼山—阴山一线最终拼合;进而推论,狼山阴山一线以北、白云鄂博—西拉木伦一线以南大片地区是古亚洲洋中的一个地体,而不是华北克拉通的一部分。古亚洲洋形成演化过程中,由北向南形成二连—贺根山(梁日暄,1994;Nozaka and Liu,2002;Xiao Wenjiao et al.,2003;Zhang Zhicheng et al.,2015)和索伦山—西拉木伦两条重要的蛇绿岩带(梁日暄,1994;王玉净和樊志勇,1997;刘建峰等,2016)。二连—贺根山蛇绿岩带为俯冲带型蛇绿岩带(Xiao Wenjiao et al.,2003),闭合时间晚于早二叠世(张磊等,2013;王金芳等,2017;张晓飞等,2018a,b,2019;程杨等,2019;范玉须等,2019;李英雷等,2021)。索伦山—西拉木伦蛇绿岩带为洋中脊蛇绿岩带(Xiao Wenjiao et al.,2003;Li Jinyi,2006;Jian Ping et al.,2008)。闭合时间为晚二叠世末—早三叠世(Xiao Wenjiao et al.,2003;Li Jinyi,2006;李朋武等,2006;李锦轶等,2007;邓胜徽等,2009;邓晋福等,2015;刘建峰等,2016)。贺根山蛇绿岩带两侧发育大规模碱性碱长(A 型)花岗岩,组成一条近东西向的花岗岩带(洪大卫等,1991;Zhang Xiaohui et al.,2014;Tong Ying et al.,2015)。花岗岩年龄集中于晚石炭世—早二叠世 271.7±0.7~297±3Ma,形成于拉伸构造环境(洪大卫等,1991;施光海等,2004;张玉清等,2009;张磊等,2013;程银行等,2014;Zhang Xiaohui et al.,2014;Tong Ying et al.,2015;肖中军等,2015;贾孝新等,2017;张晓飞等,2018)。阿巴嘎旗阿德拉嘎碱长花岗岩为首次发现(河北省区域地质矿产调查研究所,2016),本文在岩石学、地球化学和同位素年代学的基础上,探讨碱长花岗岩岩石成因和构造环境为区域碱性(A 型)花岗岩带对比研究提供资料。

1 区域地质背景和岩石学特征

研究区位于位于中亚造山带(CAOB)东南部,贺根山蛇绿岩带北侧,隶属于乌里雅斯太活动陆缘(图 1a)。

区域出露地层包括奥陶系、石炭系和第四系(图 1b)(河北省区域地质矿产调查研究所,2016)。奥陶系出露地层为下奥陶统铜山组、中奥陶统多宝山组和中—上奥陶统裸河组。铜山组岩性主要为变质中粗粒长石岩屑砂岩、变质细粒岩屑砂岩、变质砾岩夹变质粉砂岩、变质安山岩和结晶灰岩,在变质岩屑长石砂岩见有腕足化石及海百合茎化石。多宝山组主要为变质玄武安山岩,杏仁状玄武安山岩夹少量变质砂岩、泥质粉砂岩。裸河组主要为变质细粒长石砂岩、长石岩屑砂岩夹变质粉砂岩、变质安山岩,变质粉砂岩中产 *Glyptograptus*(矮小雕笔石)化石。石炭系出露地层为上石炭统宝力高庙组,岩性主要为红柱石角岩化粉砂岩、细粒岩屑砂岩、粗粒岩屑砂岩、砾岩、英安质角砾熔结凝灰岩、安山岩、流纹岩等。第四系包括更新统阿巴嘎组和全新统冲洪积物。阿巴嘎组岩性为气孔、杏仁状玄武岩、橄榄玄武岩、玄武质集块角砾岩、玄武质浮岩。冲洪积物由砂砾、砂、黏土等组成。

侵入岩较为发育,岩性主要为二长花岗岩、正长花岗岩、阿德拉嘎碱长花岗岩和花岗斑岩等,岩体均形成于晚石炭世。

阿德拉嘎碱长花岗岩分布于阿德拉嘎附近,呈不规则状产出,长轴方向近东西向,岩石坚硬,节理裂隙发育,一组节理走向北东 20°,另一组节理走向北西 70°,倾角 85°,出露面积约为 13km^2。岩体内部原生节理发育,局部节理有赤—磁铁矿薄膜充填。该岩体侵入晚石炭世二长花岗岩及正长花岗岩之中,被更新世阿巴嘎组玄武岩角度不整合覆盖。(图 2a)。

阿德拉嘎碱长花岗岩新鲜面呈肉红色,具细粒花岗结构,块状构造(图 2b)。岩石由钾长石、斜长石、石英组成。钾长石为条纹长石,半自形—近自形板状,粒径 0.1~1.5 mm,具高岭土化,轻微绢云母化,含量 60%~70%。斜长石呈半自形板状,粒径为 0.1~0.8 mm,零散状分布,斜长石牌号 $An=27$,为更长石,含量 0%~5%。石英呈半自形—它形粒状,粒径为 0.1~1.8 mm,半自形粒状石英多呈堆状聚集分布,它形粒状石英呈填隙状分布,具轻微波状消光,含量 30%~35%。

区内断裂较为发育,以北东向、北西向为主,近东西向及南北向次之。形成时代最早追溯到加里东期,最晚至更新世阿巴嘎期。

2 样品采集和实验方法

系统地质调查的基础上选择新鲜具有代表性样品进行岩石学、地球化学、同位素年代学测试,样品位置及编号见图 1b,其中地球化学数据样品 6 件,编号为 P3YQ1、P3YQ2、P3YQ3、P3YQ4、P3YQ5、P3YQ6,同位素样品 1 件,编号为 P3TW,采样位置与 P3YQ3 位置相同。

样品地球化学分析由河北省区域地质矿产调查

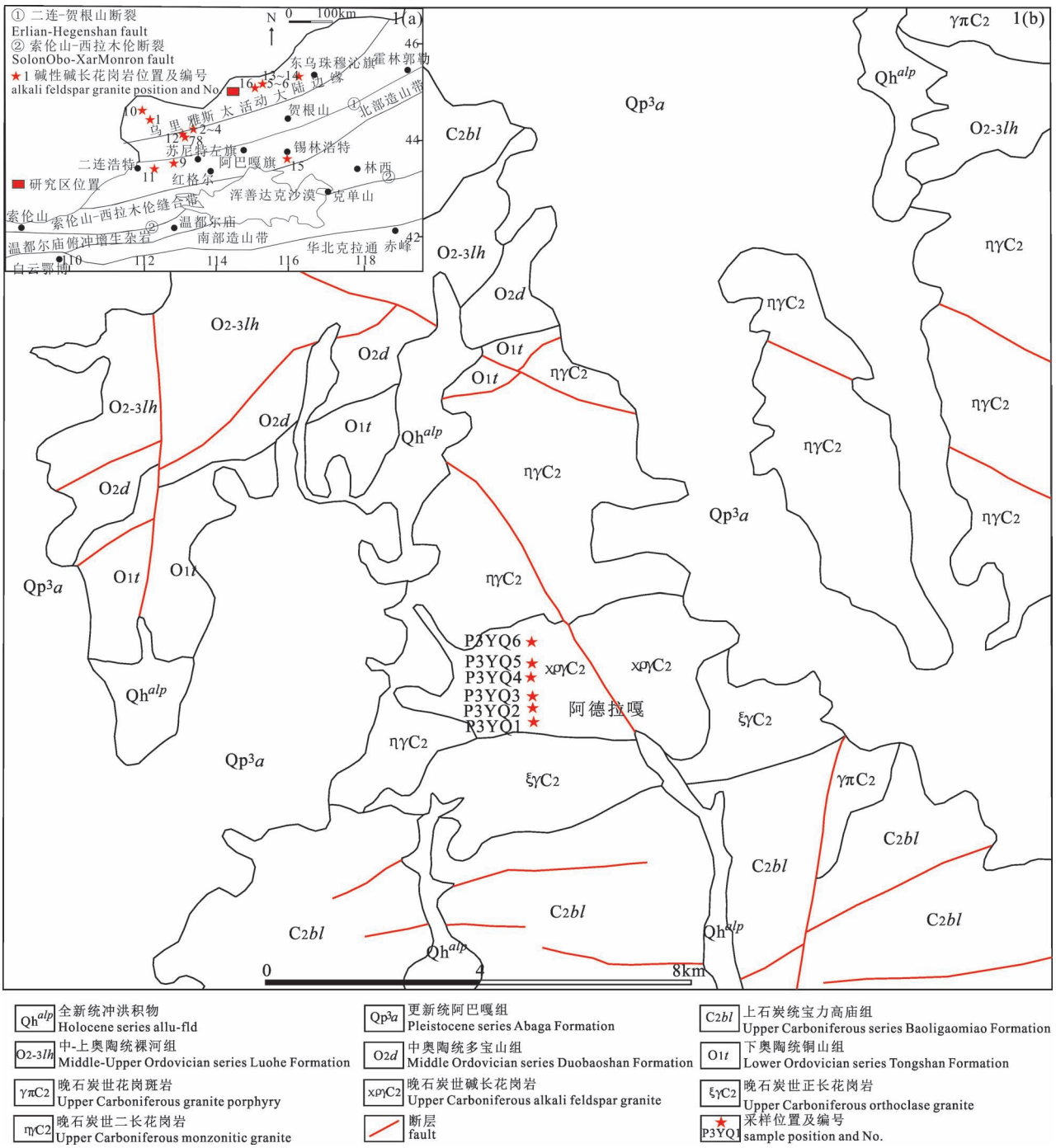

图 1（a）阿巴嘎旗阿德拉嘎碱长花岗岩区域构造简图;（b）阿德拉嘎碱长花岗岩地质简图
（河北省区域地质矿产调查研究所,2016）

Fig. 1（a）Sketch tectonic map（a）and geoloical map（b）of the Adelaga alkali feldspar granite, in Abaga Banner, Inner Mongolia(Hebei Institute of Regional Geology and Mineral Resuorces, 2016)

图 1a 中数据来源：1—焦天佳,2015;2~3—肖中军等,2015;4—Zhang Xiaohui et al.,2014; 5—刘建峰等,2009;6—张玉清等,2009;7—Zhang Xiaohui et al.,2014; 8~11—Tong Ying et al.,2015; 12—贾孝新等,2017;13~14—程银行等,2014;15—施光海等,2004;16—石文杰等,2019

Data of the Fig. 1a from: :1—Jiao Tianjia,2015&;2~3—Xiao Zhongjun et al.,2015&;4—Zhang Xiaohui et al.,2014; 5—Liu Jianfeng et al.,2009&;6—Zhang Yuqing et al.,2009&;7—Zhang Xiaohui et al.,2014; 8~11—Tong Ying et al.,2015; 12—Jia Xiaoxin et al.,2017&;13~14—Cheng Yinhang et al.,2014&;15—Shi Guanghai et al.,2004&;16—Shi Wenjie et al.,2019&

图 2 阿德拉嘎碱长花岗岩野外照片(a)及显微照片(b)

Fig. 2 Filedphotographs(a) and Microphotographs of the Adelaga alkali-feldspar granite

Kfs—钾长石;Qtz—石英

Kfs—K-feldspar;Qtz—quartz

研究所实验室完成。主量元素分析(SiO_2、TiO_2、Al_2O_3、Fe_2O_3、MgO、MnO、Na_2O、K_2O、CaO、P_2O_5)采用 X 射线荧光光谱(XRF)完成,分析测试仪器为 Axios^{max}X 射线荧光光谱仪,检测依据为《GB/T14506.28-2010》;灼失量分析采用重量法完成,检测依据《DZG20-1》;H_2O^-分析采用重量法完成,检测依据《GB/T14506.1-2010》;H_2O^+分析采用重量法完成,检测依据《GB/T14506.2-2010》,灼失量、H_2O^-、H_2O^+采用 P1245 电子分析天平测试;FeO 采用 50mL 滴定管滴定,检测依据为《GB/T14506.14-2010》,主量元素、灼失量、H_2O^-、H_2O^+分析精度为 0.05%。稀土元素及微量元素采用离子体质谱,检测依据为《DZG20-1》,分析测试仪器为 X Serise2 等离子体质谱仪,稀土元素分析绝对误差为 0.1×10^{-6},微量元素≤5×10^{-6}。实验温度为 20℃,湿度为 30%。

锆石挑选由河北省区域地质矿产调查研究所实验室完成。样品经过常规的分选后,在双目镜下经人工挑选出纯度在 99%以上的锆石,选出的锆石完整、透明度高。将挑选好的锆石粘贴在环氧树脂表面,打磨抛光后露出锆石表面,制成靶样。锆石透、反射光及阴极荧光(CL)照相,由北京锆年领航科技有限公司实验室完成,仪器为 JEOL 公司生产的 JSM6510 型扫描电子显微镜。

锆石 MC-ICP-MS 年龄测试在中国地质科学院矿产资源研究所 MC-ICP-MS 实验室完成。锆石定年分析所用仪器为 Finnigan Nepture 型 MC-ICP-MS,激光剥蚀系统为 GeoLas 2005。激光剥蚀束斑直径为 25μm,剥蚀深度为 20~40 μm,频率为 10 Hz,能量密度为 2.5 J/cm^2,剥蚀过程中采用氦气载气,氩气补偿。信号较小的^{207}Pb、^{206}Pb、^{204}Pb(^{+204}Hg)、^{202}Hg 用离子计数器(multi-ion-counters)接收,^{208}Pb、^{232}Th、^{238}U 信号用法拉第杯接收,实现了所有目标同位素信号的同时接收,并且不同质量数的峰基本平坦,进而获得高精度数据。测试过程中在每测定 10 个锆石样品前后重复测定 2 个锆石 GJ1 对样品进行校正,并测量 1 个锆石 Plesovice,用于观测仪器的状态确保测试精确度。详细实验过程见侯可军等(2009)。实验温度 20℃,实验湿度 55%。对采集的数据采用中国地质大学刘勇胜博士研发的 ICP-Ms DataCal 程序(Liu Yongsheng et al.,2008)和 Ludwig(2012) 的 Isoplot 程序进行处理,并绘制谐和图等图件,置信度为 95%。

3 测试结果

3.1 主量元素

阿德拉嘎碱长花岗岩样品烧失量(0.29%~0.69%)较低,总量为 99.97%~99.98%,岩石地球化学特征能够有效反应岩石特征(表 1)。样品 SiO_2 质量分数为 77.12%~77.75%,变化范围较小,含量较高,为酸性岩;TiO_2 为 0.06%~0.08%,含量较低;Al_2O_3 为 12.36%~12.53%,变化范围较小;Fe_2O_3 为 0.88%~1.02%;MgO 为 0.02%~0.05%,含量较低;K_2O 为 3.87%~4.48%;Na_2O 质量分数为 3.96%~

4.36%,含量较高;Na_2O+K_2O 为 8.07%~8.61%。阿德拉嘎碱长花岗岩 TAS 图解中,样品投点于花岗岩区域,属于亚碱性系列(图 3a)。阿德拉嘎碱长花岗岩 QAP 图解中样品投点于碱长花岗岩区域(图 3b)。K_2O—SiO_2 图解(图 3c)中样品投点于高钾钙碱性系列区域。岩石分异指数 DI 为 96.75~97.41,分异程度较高,铝饱和指数 A/CNK 为 1.03~1.09,为弱过铝质岩石。

3.2　稀土元素

样品稀土总量(ΣREE)为 59.46×10^{-6}~162.29×10^{-6},含量较低,变化范围较大,轻稀土 LREE 含量为 27.35×10^{-6}~124.23×10^{-6},重稀土 HREE 含量为 27.89×10^{-6}~38.06×10^{-6}(表 1)。轻、重稀土 LREE/HREE 比值为 0.85~3.97,$(La/Yb)_N$ 为 0.26~2.09,$(Ce/Yb)_N$ 为 3.09~14.44,轻重稀土分异程度较低;$(La/Sm)_N$ 为 1.17~2.59,轻稀土分异程度较低;$(Gd/Yb)_N$ 为 0.22~0.68,重稀土分异程度较低;δEu 为 0.15~0.37,负异常明显;δCe 为 0.84~8.20,整体具弱正异常。稀土配分曲线呈海鸥型,轻重稀土分异程度均较低(图 4a)。

3.3　微量元素

与天山—兴蒙造山系碱长花岗岩(迟清华和鄢明才,2007)相比,样品具有高 Hf、Nb,低 Ba、Sr、U,中等 Rb、Ta、Th、Ga、Zr 特征。样品微量元素蛛网图配分曲线一致(图 4b),具有明显 Ba、Sr、P、Ti 负异常。

3.4　锆石 U-Pb 年龄

阿德拉嘎碱长花岗岩用于测试的锆石自形程度较好,呈长柱状,发育振荡环带,具岩浆成因特征(Rubatto and Gebauer,2000)。阿德拉嘎碱长花岗岩

表 1 阿德拉嘎碱长花岗岩主量元素(%)、稀土元素($\times10^{-6}$)、微量元素($\times10^{-6}$)组成

Table 1 Major element(%),REE ($\times10^{-6}$) and trace element($\times10^{-6}$) compositions of the Adelaga alkali feldspar granite

	P3YQ1	P3YQ2	P3YQ3	P3YQ4	P3YQ5	P3YQ6	*		P3YQ1	P3YQ2	P3YQ3	P3YQ4	P3YQ5	P3YQ6	*
SiO_2	77.36	77.23	77.31	77.12	77.75	77.15	75.26	Eu	0.36	0.32	0.30	0.32	0.13	0.16	0.40
Al_2O_3	12.42	12.44	12.40	12.47	12.36	12.53	12.98	Gd	5.17	2.89	3.88	5.89	2.35	2.75	5.6
Fe_2O_3	0.99	0.96	0.88	1.02	0.95	0.88	0.90	Tb	1.03	0.84	0.92	1.28	0.86	0.85	0.59
FeO	0.07	0.06	0.17	0.05	0.05	0.05	0.46	Dy	7.40	7.75	7.12	9.62	8.24	7.83	
MnO	0.004	0.008	0.004	0.005	0.005	0.003	0.03	Ho	1.56	1.91	1.61	2.13	2.05	1.90	
TiO_2	0.07	0.08	0.07	0.06	0.07	0.07	0.16	Er	4.79	6.32	5.12	6.78	6.73	6.23	
CaO	0.16	0.15	0.15	0.30	0.16	0.16	0.47	Tm	0.98	1.31	1.09	1.46	1.41	1.35	
MgO	0.03	0.04	0.02	0.04	0.05	0.05	0.14	Yb	6.24	8.06	6.89	9.23	8.91	8.62	2.9
Na_2O	4.13	4.13	4.12	4.36	4.20	3.96	3.71	Lu	1.15	1.46	1.26	1.67	1.56	1.57	0.45
K_2O	4.41	4.48	4.43	4.06	3.87	4.41	4.64	Y	41.25	56.46	44.13	63.64	58.83	56.02	23
P_2O_5	0.039	0.018	0.036	0.012	0.012	0.021	0.04	ΣREE	140.89	80.75	103.10	162.29	59.46	109.51	
烧失	0.29	0.38	0.38	0.50	0.50	0.69		LREE	112.57	50.21	75.21	124.23	27.35	78.41	
总量	99.97	99.97	99.98	99.97	99.97	99.97		HREE	28.32	30.54	27.89	38.06	32.11	31.10	
Q	36.1	35.7	36.09	35.52	38.13	36.98		LREE/HREE	3.97	1.64	2.70	3.26	0.85	2.52	
An	0.54	0.63	0.51	1.42	0.72	0.66		$(La/Yb)_N$	2.09	0.84	1.24	2.03	0.26	0.27	
Ab	35.08	35.11	35.02	37.1	35.74	33.77		$(Ce/Yb)_N$	14.44	5.34	9.12	9.04	3.09	12.75	
Or	26.16	26.6	26.3	24.13	23	26.26		$(La/Sm)_N$	1.88	2.59	1.92	2.42	1.36	1.17	
C	0.66	0.57	0.64	0.39	1.01	1.01		$(Gd/Yb)_N$	0.68	0.30	0.46	0.52	0.22	0.26	
Hy	0.55	0.54	0.52	0.61	0.6	0.54		δEu	0.19	0.37	0.23	0.15	0.21	0.22	
DI	97.33	97.4	97.41	96.75	96.88	97		δCe	1.23	1.34	1.34	0.84	2.19	8.20	
A/CNK	1.06	1.05	1.05	1.03	1.09	1.09		Ba	15.0	23.1	15.5	42.6	51.0	40.1	325
SI	0.31	0.42	0.21	0.42	0.55	0.54		Hf	8.40	9.43	8.12	8.25	8.79	8.36	5.4
AR	4.82	4.82	4.82	4.87	4.63	4.32		Nb	18.26	18.40	18.28	22.08	20.86	25.87	16.0
R1	2635	2613	2633	2624	2770	2696		Rb	164.4	153.5	163.7	145.2	121.4	154.1	160
R2	263	263	261	280	264	267		Sr	7.7	8.9	7.3	14.3	12.9	13.0	70
La	18.19	9.49	11.92	26.16	3.20	3.21	29	Ta	1.58	1.92	1.55	1.49	1.43	1.98	1.56
Ce	55.16	26.34	38.45	51.08	16.83	67.26	63	Th	17.61	17.94	14.54	21.49	17.81	21.56	16.9
Pr	6.65	2.46	4.13	8.40	1.11	1.26		U	1.86	2.01	1.85	2.41	1.99	1.88	2.74
Nd	25.97	9.23	16.41	31.31	4.56	4.75	22	Ga	20.32	19.86	19.95	21.07	17.60	20.37	18
Sm	6.24	2.37	4.00	6.96	1.52	1.77	4.1	Zr	187.5	208.3	181.0	185.9	196.5	183.9	160

注:*为天山-兴安造山系碱长花岗岩,数据来源于(迟清华和鄢明才,2007)。Alkali-feldspar granite of the Ten-zan-Khingan Orogenic System, based on data from (Chiqinghua and Yan Mingcai,2007).

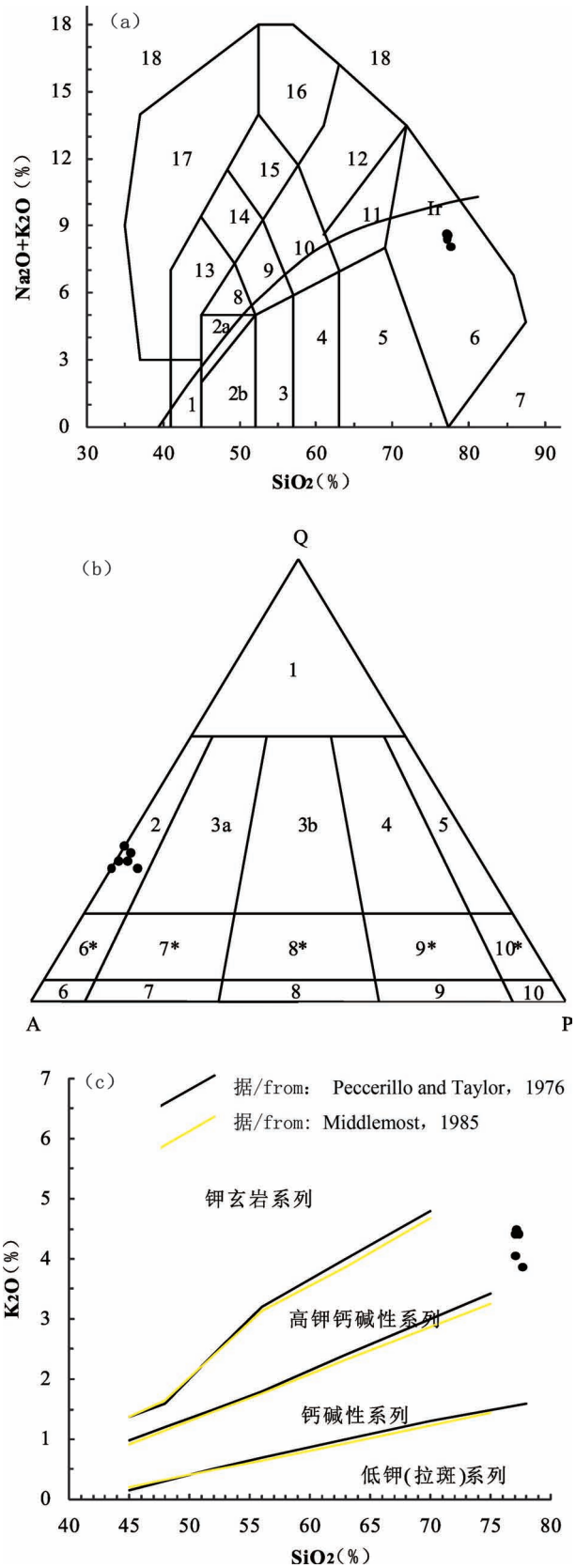

图 3 阿德拉嘎碱长花岗岩 TAS 图解(a)(底图据 Middlemost,1994)、QAP 图解(b)(底图具 Streckeisen,1976)、$K_2O—SiO_2$ 图解(c)(底图据 Middlemost,1994)

Fig. 3 TAS diagram (a) (after Middlemost, 1994), QAP diagram (b) (after Streckeisen, 1976) and $K_2O—SiO_2$ diagram (c) (after Middlemost, 1994) of the Adelaga alkali-feldspar granite

(a) Ir—Irvine 分界线,上方为碱性,下方为亚碱性(Irvine and Baragar, 1971)。1—橄榄辉长岩;2a—碱性辉长岩;2b—亚碱性辉长岩;3—辉长闪长岩;4—闪长岩;5—花岗闪长岩;6—花岗岩;7—硅英岩;8—二长辉长岩;9—二长闪长岩;10—二长岩;11—石英二长岩;12—正长岩;13—副长石辉长岩;14—副长石二长闪长岩;15—副长石二长正长岩;16—副长正长岩;17—副长深成岩;18—霓方钠岩/磷霞岩/粗白榴岩

(b) 1—富石英花岗岩;2—碱长花岗岩;3a—花岗岩;3b—花岗岩(二长花岗岩);4—花岗闪长岩;5—英云闪长岩、斜长花岗岩;6*—碱长石英正长岩;7*—石英正长岩;8*—石英二长岩;9*—石英二长闪长岩;10*—石英闪长岩、石英辉长岩、石英斜长岩;6—碱长正长岩;7—正长岩;8—二长岩;9—二长闪长岩、二长辉岩;10—闪长岩、辉长岩、斜长岩

锆石阴极荧光(CL)图像显示(图 5),锆石图像较暗,Th、U 含量略高。选择不发育裂隙和包裹体的锆石进行年龄测试,在发育振荡环带的位置打点。锆石 Pb 含量 $5.351\times10^{-6}\sim130.3\times10^{-6}$,Th 含量 $59.81\times10^{-6}\sim1627\times10^{-6}$,U 含量 $89.72\times10^{-6}\sim1525\times10^{-6}$(表 2)。本样品锆石 Th/U 比值 0.49~1.07>0.4,与变质成因锆石(Th/U≤0.1)差异明显,表明锆石为为岩浆成因锆石(Hoskin and Black,2000;Rubatto and Gebauer, 2000; Hoskin and Schaltegger, 2003; Cleasson et al.,2000;Belousova et al.,2002)。本样品 U-Pb 年龄<1.0 Ga,因而采用锆石 $^{206}Pb/^{238}U$ 年龄(Griffin et al.,2004)。样品锆石 $^{206}Pb/^{238}U$ 分析点呈点群分布,分布较为集中,年龄值为 294.9±3.2~316.2±3.1 Ma(图 6a),加权平均值为 310.7±2.6 Ma,MSWD=2.5(图 6b),表明岩体形成于晚石炭世。

4 讨论

4.1 年代学意义

贺根山蛇绿岩带两侧发育大规模碱性(A 型)花岗岩带(洪大卫等,2000;张磊等,2013;Zhang Xiaohui et al.,2014;张晓飞等,2018a)。查干敖包碱长花岗岩(A 型)锆石 U-Pb 年龄为 312.2±7.4Ma(焦天佳,2015)。阿尔善布拉格细粒碱性花岗岩锆石 U-Pb 年龄为 295.8±1.4(肖中军等,2015),中粗粒碱性花岗岩锆石 U-Pb 年龄 297±3Ma(肖中军等,

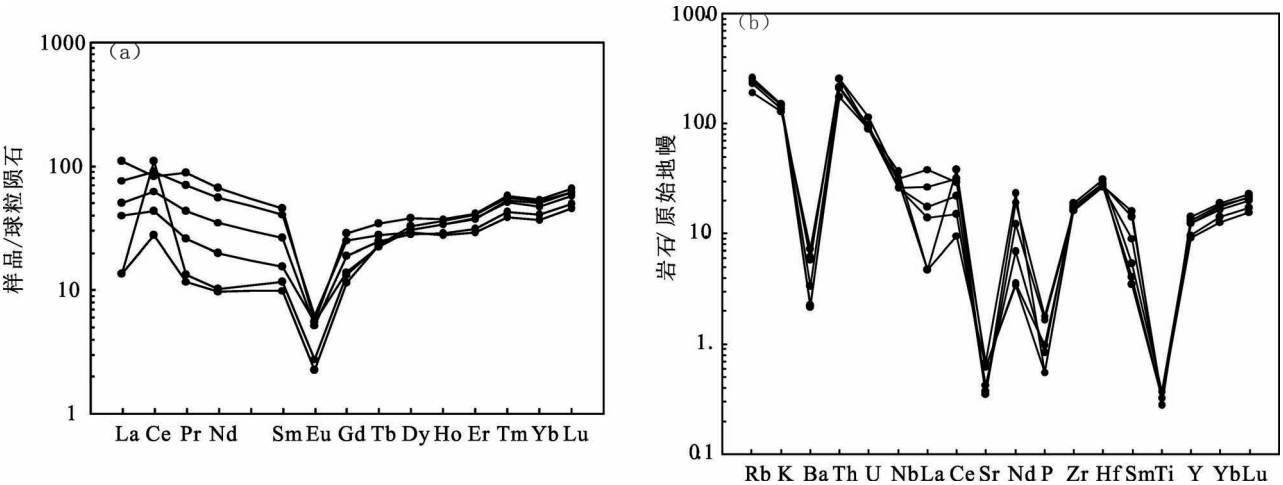

图 4 阿德拉嘎碱长花岗岩稀土元素球粒陨石标准化分布型式图(a)和微量元素原始地幔标准化蛛网图(b)(标准化数据据 Sun and Mcdonough,1989)

Fig. 4 Chondrite normalized REE patterns(a) and primitive mantle normalized trace elements spider diagram of the Adelaga alkali-feldspar granite(modified after Sun and Mcdonough,1989)

2015),碱性花岗岩锆石 U-Pb 年龄为 288.3±2.3~290.0±2.2Ma(Zhang Xiaohui et al.,2014)。京格斯台中粗粒碱长花岗岩(A 型)锆石 U-Pb 年龄为 295±2.8Ma(刘建峰等,2009),碱性花岗岩锆石 U-Pb 年龄为 284.8±1.1Ma(张玉清等,2009)。白音乌拉碱性花岗岩锆石 U-Pb 年龄为 290±2.6Ma(Zhang

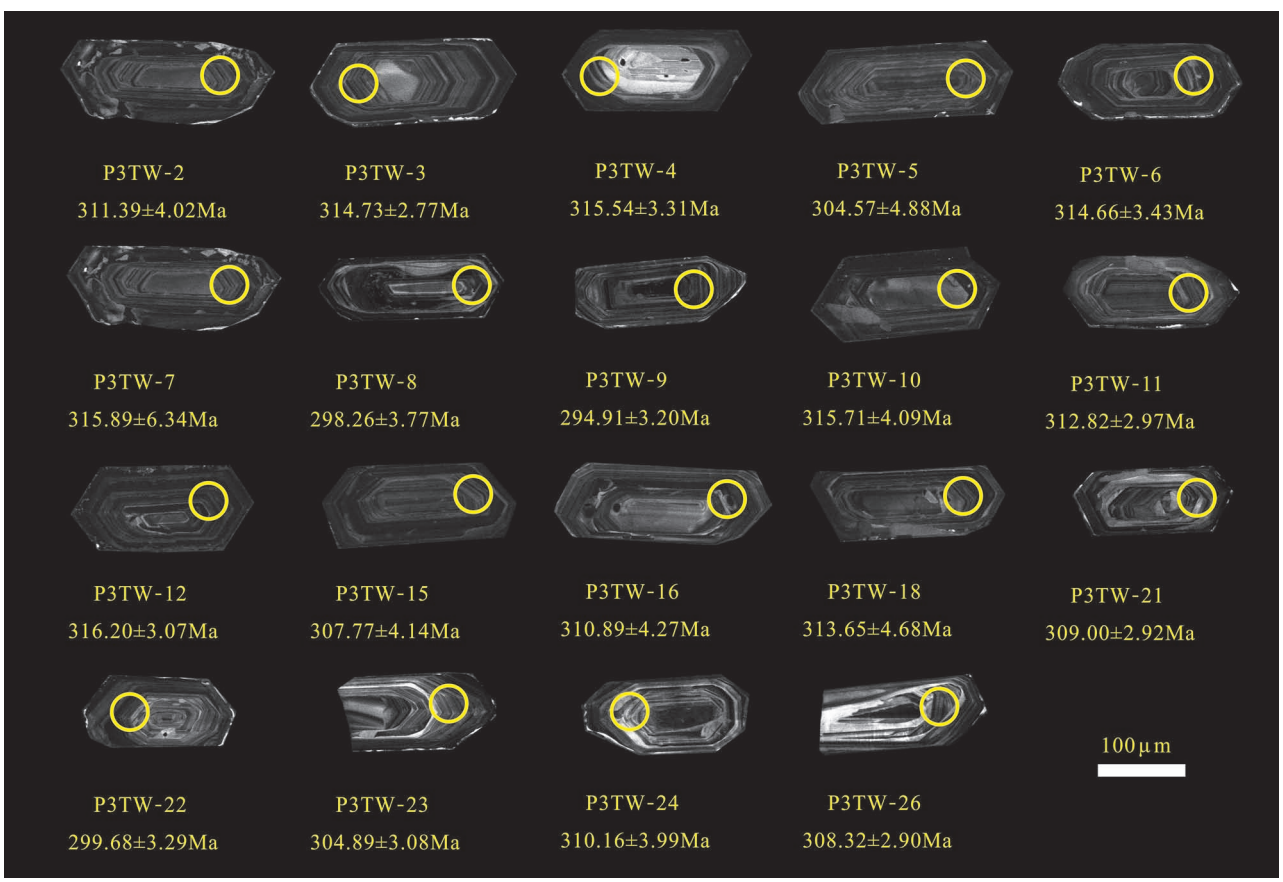

图 5 阿德拉嘎碱长花岗岩锆石阴极荧光(CL)照片

Fig. 5 Zircons cathodoluminescence (CL) images of the Adelaga alkali-feldspar granite

表 2 阿德拉嘎碱长花岗岩(P3TW)LA-ICP-MS 锆石同位素分析结果

Table 2 Zircon LA-ICP-MS analytical results of of the Adelaga alkali feldspar granite (P3TW)

测点号	元素含量($\times10^{-6}$)			Th/U	同位素比值						同位素年龄(Ma)						谐和度(%)
	Pb	Th	U		$n(^{207}Pb)/n(^{206}Pb)$		$n(^{207}Pb)/n(^{235}U)$		$n(^{206}Pb)/n(^{238}U)$		$n(^{207}Pb)/n(^{206}Pb)$		$n(^{207}Pb)/n(^{235}U)$		$n(^{206}Pb)/n(^{238}U)$		
					测值	1σ	测值	1σ	测值	1σ	测值	1σ	测值	1σ	测值	1σ	
P3TW-2	69.53	958.7	1217	0.79	0.05160	0.0009	0.3521	0.0060	0.04949	0.0006	267.7	40.8	306.3	5.2	311.4	4.0	95%
P3TW-3	55.73	650.9	981.9	0.66	0.05326	0.0016	0.3674	0.0064	0.05003	0.0004	339.8	68.8	317.7	5.5	314.7	2.8	98%
P3TW-4	63.75	719.3	1110	0.65	0.05364	0.0023	0.3710	0.0081	0.05017	0.0005	356.0	98.8	320.4	7.0	315.5	3.3	97%
P3TW-5	30.99	390.8	578.4	0.68	0.05781	0.0020	0.3857	0.0065	0.04838	0.0008	522.7	74.2	331.2	5.6	304.6	4.9	98%
P3TW-6	5.351	59.81	89.72	0.67	0.05629	0.0085	0.3882	0.0232	0.05002	0.0005	463.6	335.1	333.1	19.9	314.7	3.4	95%
P3TW-7	83.40	938.3	1386	0.68	0.05340	0.0057	0.3698	0.0523	0.05022	0.0010	345.8	243.2	319.5	45.2	315.9	6.3	97%
P3TW-8	42.77	487.9	762.0	0.64	0.05812	0.0102	0.3795	0.0616	0.04735	0.0006	534.5	384.2	326.7	53.0	298.3	3.8	96%
P3TW-9	60.85	702.0	1130	0.62	0.05902	0.0023	0.3809	0.0075	0.04681	0.0005	567.9	84.4	327.7	6.5	294.9	3.2	98%
P3TW-10	69.28	781.6	1227	0.64	0.05400	0.0021	0.3736	0.0095	0.05019	0.0007	370.1	87.1	322.3	8.2	315.7	4.1	99%
P3TW-11	54.81	654.2	962.5	0.68	0.05566	0.0018	0.3816	0.0074	0.04972	0.0005	438.8	72.8	328.2	6.4	312.8	3.0	95%
P3TW-12	78.71	1045	1315	0.79	0.05530	0.0015	0.3833	0.0078	0.05027	0.0005	424.4	60.4	329.5	6.8	316.2	3.0	98%
P3TW-15	36.25	389.0	679.6	0.57	0.05695	0.0011	0.3840	0.0063	0.04890	0.0007	489.6	42.6	323.0	5.4	307.8	4.1	97%
P3TW-16	43.68	618.9	771.7	0.80	0.05230	0.0013	0.3563	0.0084	0.04941	0.0007	298.7	56.2	309.5	7.3	310.9	4.3	96%
P3TW-18	130.3	1627	1525	1.07	0.05429	0.0048	0.3732	0.0389	0.04986	0.0007	383.2	200.5	322.1	33.6	313.7	4.7	99%
P3TW-21	20.08	306.7	361.1	0.85	0.05541	0.0021	0.3752	0.0069	0.04910	0.0005	429.1	82.6	323.5	6.0	309.0	2.9	99%
P3TW-22	84.54	744.1	1508	0.49	0.05368	0.0032	0.3522	0.0136	0.04759	0.0005	357.6	134.0	306.4	11.8	299.7	3.3	98%
P3TW-23	71.53	983.6	1298	0.77	0.05429	0.0014	0.3626	0.0061	0.04843	0.0005	383.2	58.7	314.1	5.3	304.9	3.1	98%
P3TW-24	55.07	744.5	971.2	0.77	0.05325	0.0022	0.3619	0.0095	0.04929	0.0006	339.6	92.3	313.6	8.3	310.2	4.0	96%
P3TW-26	86.51	1374	1447	0.95	0.05561	0.0025	0.3756	0.0081	0.04899	0.0005	436.8	99.0	323.8	7.0	308.3	2.9	95%

Xiaohui et al., 2014), 285±1Ma (Tong Ying et al., 2015)。宝拉格碱性花岗岩锆石 U-Pb 年龄为 285±1.1Ma (Tong Ying et al., 2015)。红格尔碱性花岗岩锆石 U-Pb 年龄为 276±1Ma(Tong Ying et al., 2015)。塞因乌苏碱性花岗岩锆石 U-Pb 年龄为 279±1 Ma (Tong Ying et al., 2015)。白音乌拉北细粒碱性花岗岩锆石 U-Pb 年龄为 280±3Ma,形成于早二叠世(贾孝新等,2017)。罕乌拉碱长花岗岩(A 型)锆石 U-Pb 年龄为 279.8±1.2Ma(张晓飞等,2018a)。扎拉嘎碱性花岗岩锆石 U-Pb 年龄为 272.3±0.7Ma 和 271.7±0.7Ma(程银行等,2014)。锡林浩特晶洞花岗岩(A 型)锆石 U-Pb 年龄为 276±2Ma(施光海等,2004)。白音图嘎碱长花岗岩(A 型)锆石 U-Pb 年龄为 294±2Ma,形成于早二叠世(石文杰等,2019)。拉抛碱长花岗岩(A 型)锆石 U-Pb 年龄为 325±3Ma(张磊等,2013)。区域资料表明碱性碱长(A 型)花岗岩带主要形成于早二叠世,少量形成于晚石炭世(表 3),本文在阿德拉嘎碱长花岗岩体中获得的 LA-ICP-MS 锆石 U-Pb 年龄为 310.7±2.6Ma,表明该岩体形成于晚石炭世,形成时间相对较早,为区域晚古生代岩浆活动在本区的响应。

4.2 岩石成因类型

阿德拉嘎碱长花岗岩手标本及镜下鉴定未见角闪石、白云母、堇青石、石榴子石等矿物,样品中 P_2O_5 含量极低,与 S 型花岗岩特征存在较大差异(Sylvester, 1998)。花岗岩具有高 Si、富碱($Na_2O+K_2O>8\%$),强烈 δEu 负异常(0.15~0.37),稀土配分曲线呈海鸥型,10000Ga/Al=2.68~3.19>2.6,表明岩体具 A 型花岗

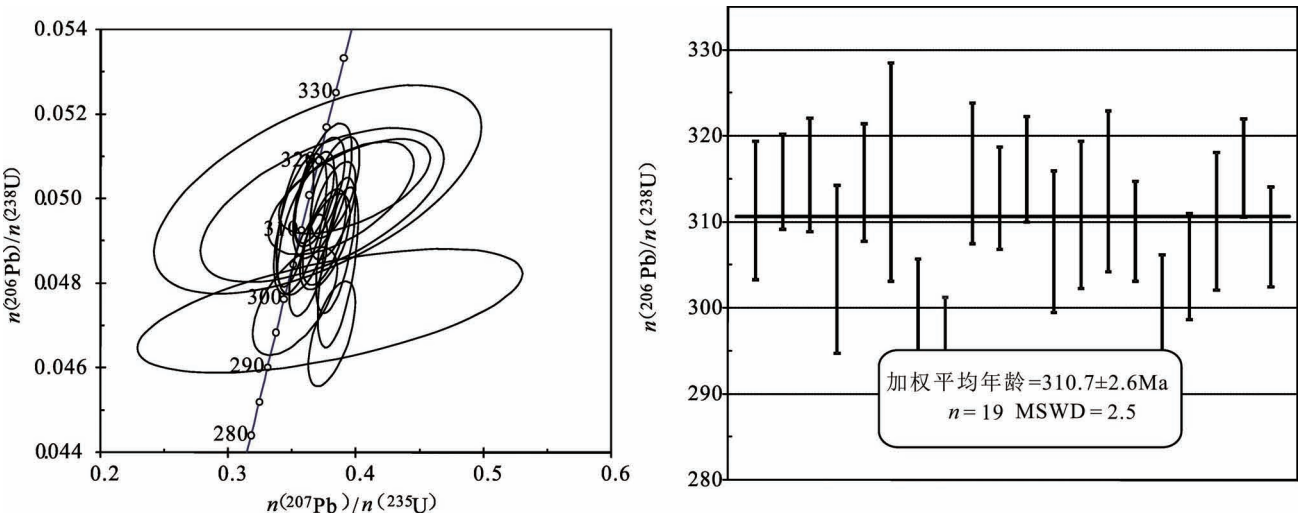

Fig. 6 U-Pb concordia diagram(a) and weighted mean ages diagram (b) of zircons of the Adelaga alkali-feldspare granite

岩的地球化学属性,与拉抛碱长花岗岩和罕乌拉碱长花岗岩等一致(Collins et al. ,1982;Whalen et al. ,1987;张磊等,2013;张晓飞等,2018a)。阿德拉嘎碱长花岗岩(Na_2O+K_2O)/CaO—(Zr+Nb+Ce+Y)图解(图 11)中样品投点于 A 型花岗岩区域。阿德拉嘎碱长花岗岩(Na_2O+K_2O)/CaO—1000Ga/Al 图解(图 12)中样品投点于 A 型花岗岩区域。岩石地球化学特征表明,阿德拉嘎碱长花岗岩的岩石成因类型为 A 型花岗岩。

花岗岩的源岩部分熔融过程中,HREE 中 Yb 主要富集于石榴子石中,Dy、Ho 主要富集于角闪石中(Sisson,1994)。岩浆源区残留相中含有少量石榴子石(10%)时,其部分熔融形成的花岗岩具有高锶低钇(adakitic)特征,并且 Y/Yb 明显大于 10(Hollocher et al. ,2002),Y/Yb 接近 10 时,源区以角闪石为主,不含或含极少石榴子石(葛小月等,2002)。阿德拉嘎碱长花岗岩 Y/Yb 比值为 6.40~7.00<10,岩浆源区以角闪石为主。δEu 强烈负异常,表明岩浆源区存在大量斜长石。综合分析认为岩浆源区残留相为角闪石+斜长石。

表 3 贺根山断裂两侧晚石炭世—早二叠世碱性碱长花岗岩

Table 3 Alkali feldspar granite and aliali granite of Upper Carboniferous epoch and Lower Permian epoch both side of the Hegenshan fault

岩体名称	岩性	年龄(Ma)	测试方法	资料来源
查干敖包	碱长花岗岩	312.2±7.4	LA-ICP-MS	焦天佳,2015
阿尔善布拉格	细粒碱性花岗岩	295.8±1.4	LA-ICP-MS	肖中军等,2015
祖横德楞	中粗粒碱性花岗岩	297±3	LA-ICP-MS	肖中军等,2015
祖横德楞	碱性花岗岩	289±2.2	LA-ICP-MS	Zhang Xiaohui et al. , 2014
京格斯台	中粗粒碱长花岗岩	295±2.8	LA-ICP-MS	刘建峰等,2009
京格斯台	碱性花岗岩	285±1	LA-ICP-MS	张玉清,2009
白音乌拉	碱性花岗岩	290±2.6	LA-ICP-MS	Zhang Xiaohui et al. , 2014
白音乌拉	碱性花岗岩	285±1	LA-ICP-MS	Tong Ying et al. , 2015
宝拉格	碱性花岗岩	285±1.1	LA-ICP-MS	Tong Ying et al. , 2015
红格尔	碱性花岗岩	276±1	LA-ICP-MS	Tong Ying et al. , 2015
塞因乌苏	碱性花岗岩	279±1	LA-ICP-MS	Tong Ying et al. , 2015
白音乌拉北	细粒碱性花岗岩	279±2.7	LA-ICP-MS	贾孝新等, 2017
扎拉嘎	碱性花岗岩	272.3±0.7	LA-ICP-MS	程银行等,2014
扎拉嘎	碱性花岗岩	271.7±0.7	LA-ICP-MS	程银行等,2014
罕乌拉	碱长花岗岩	279.8±1.2	LA-ICP-MS	张晓飞等,2018a
锡林浩特	晶洞花岗岩	276±2	LA-ICP-MS	施光海等,2004
白音图嘎	碱长花岗岩	294±2	LA-ICP-MS	石文杰等,2019
拉抛	碱长花岗岩	325±3	LA-ICP-MS	张磊等,2013

4.3　构造环境及地质意义

高场强元素(HFSE)受后期作用影响较小,能够有效判别岩石形成的构造环境(Pearce et al. ,1984)。Rb、Y(Yb)、Nb(Ta)等能够有有效区分大洋脊花岗岩(ORG)、火山弧花岗岩(VAG)、板内花岗岩(WPG)和碰撞带花岗岩(Syn-COLG)等(Pearce et al. ,1984)。Eby(1992)将 A 型花岗岩分为与洋岛玄武岩(OIB)类似,具有很低 Y/Nb,Yb/Ta 值的 A_1 型;与岛弧玄武岩(IAB)类似,具有高 Y/Nb,

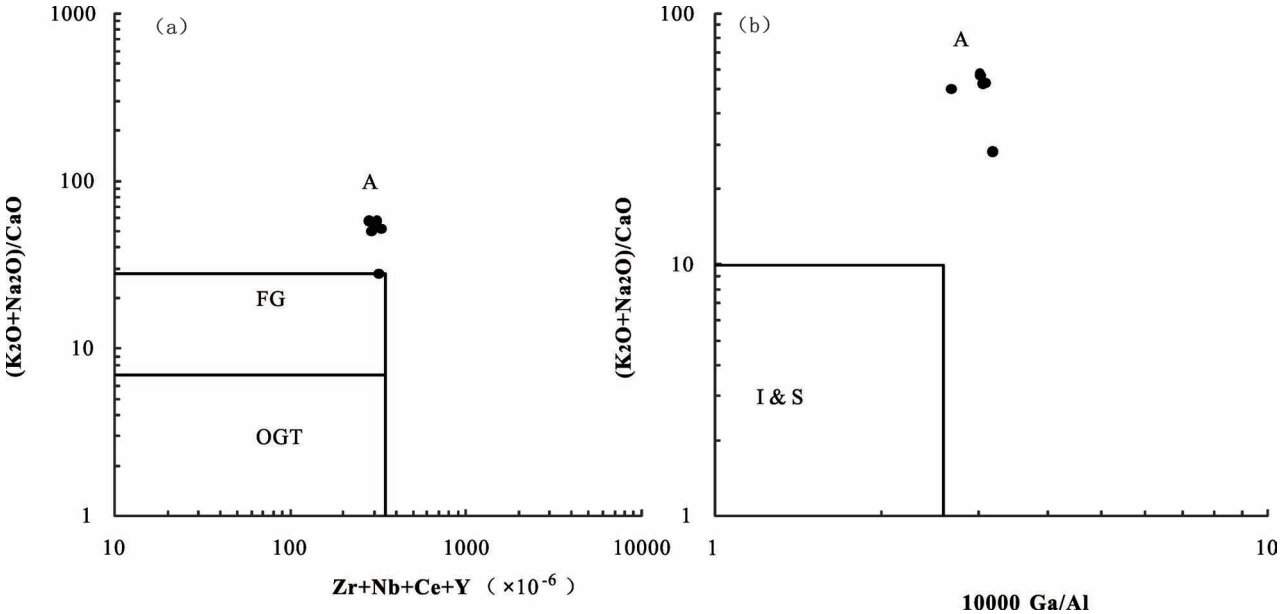

图 7 阿德拉嘎碱长花岗岩(Na_2O+K_2O)/CaO—Zr+Nb+Ce+Y 图解(a)和
(Na_2O+K_2O)/CaO—1000Ga/Al 图解(b)(底图具(Whalen et al. ,1987))

Fig. 7 Na_2O+K_2O)/CaO—Zr+Nb+Ce+Y diagram(a) and Na_2O+K_2O)/CaO—1000Ga/Al diagram(b) of the Adelaga alkali feldspar granite(modified after Whalen et al. , 1987)

Yb/Ta 值的 A_2 型。阿德拉嘎碱长花岗岩的 Y/Nb 值为 2.17 ~ 3.07,平均 3.12;Yb/Ta 值为 3.95 ~ 6.23,平均 5.87,都明显>1,显示具岛弧玄武岩亲缘性。在 Nb—Y—3Ga 和 Nb—Y—3Ce 构造环境判别图解上(图 8a,b),阿德拉嘎碱长花岗岩落在 A_2 型花岗岩区域。阿德拉嘎碱长花岗岩 Rb—Y+Nb 图解(图 9)样品投点于伸展构造背景(Pearce et al. , 1984)。

迪彦庙蛇绿岩枕状玄武岩锆石 U-Pb 年龄为 333.4±8.5Ma,形成于俯冲环境(李英杰等,2018)。跃进地区花岗岩类锆石 U-Pb 年龄为 310 ~ 330Ma,具岛弧侵入岩特征,形成于俯冲背景下(王树庆等,

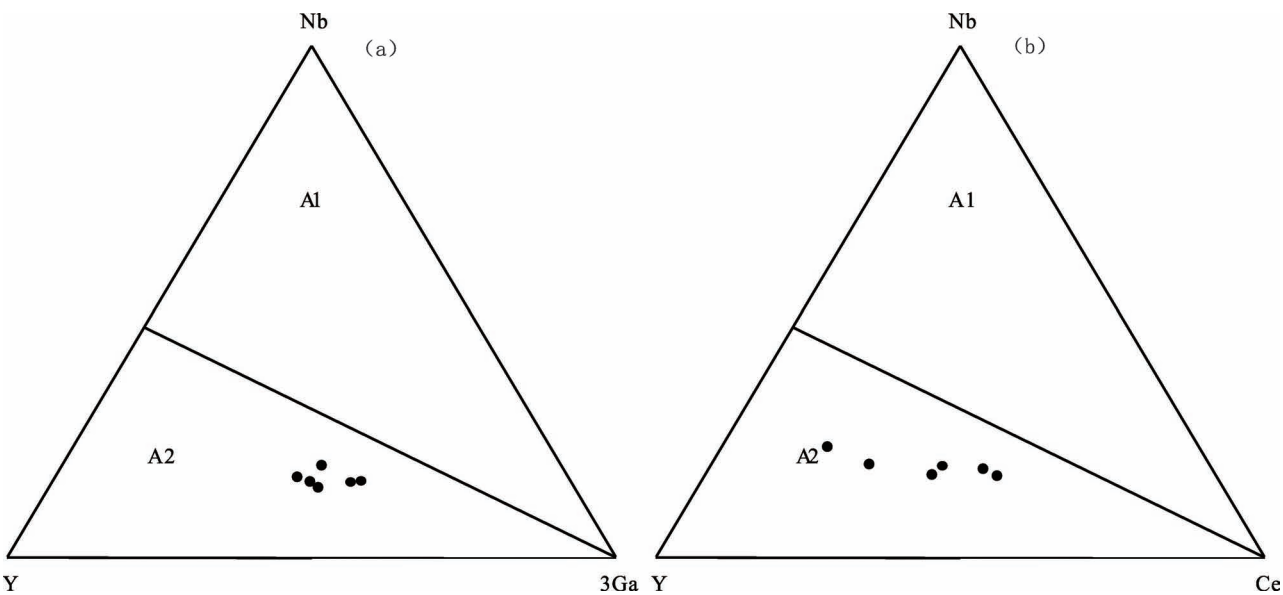

图 8 阿德拉嘎碱长花岗岩 Nb—Y—3Ga 图解(a)和 Nb—Y—Ce 图解(b)(底图具 Eby,1992)

Fig. 8 Nb—Y—3Ga diagram(a) and Nb—Y—Ce diagram(b) of the Adelaga alkali feldspar granite(modified after Eby, 1992)

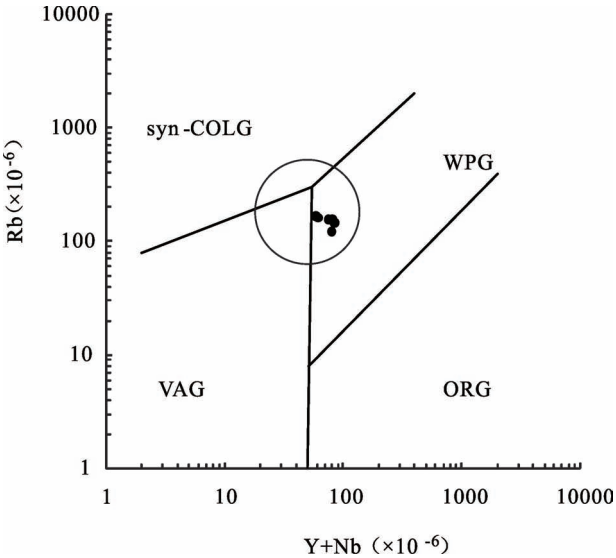

图 9 阿德拉嘎碱长花岗岩 Rb—(Y+Nb)图解
(Pearce et al. ,1984)

Fig. 9 Rb—(Y+Nb) diagram of the Adelaga alkali feldspar granite (modified after Pearce et al. ,1984)

2018)。迪彦庙—达青蛇绿岩斜长花岗岩锆石 U-Pb 年龄为 330. 1±3. 2Ma、316. 5±2. 4Ma,辉长岩、高镁闪长岩锆石 U-Pb 年龄分别为 286. 1±6. 1Ma、283. 7±4. 7Ma,结合地球化学和 Hf 同位素数据,区域石炭纪—二叠纪处于洋盆扩张—洋内俯冲阶段(程杨等,2019,2020)。苏尼特右旗蛇绿岩带中发育英云闪长岩,锆石 U-Pb 年龄为 322. 3±5. 2Ma,具高锶低钇(adakitic)特征,表明古亚洲洋晚石炭世仍在俯冲(董培培等,2021)。迪彦庙孜来可图岩体锆石 U-Pb 年龄为 322. 2±1. 3Ma,形成于古亚洲洋俯冲环境(范玉须等,2020)。巴彦都兰角闪石岩锆石 U-Pb 年龄为310±1Ma,地球化学结合电子探针和 Hf 同为研究认为,其形成于古亚洲洋俯冲背景下(张夏炜等,2021)。梅劳特乌拉 SSZ 型蛇绿岩呼和德花岗闪长岩 U-Pb 年龄分别为 294. 4±1. 7Ma,呼都格奥长花岗岩锆石 U-Pb 年龄分别为 306. 3±1. 9Ma 和 315. 5±1. 9Ma,白音呼舒奥长花岗岩锆石 U-Pb 年龄为 309. 2±1. 6Ma,均具高锶低钇(adakitic)特征;蛇绿岩中高镁安山岩锆石 U-Pb 年龄 315. 0±2. 3Ma,形成于古亚洲洋俯冲环境(王金芳等,2017,2019,2020,2021)。沙巴尔吐蛇绿构造混杂岩超镁铁质岩和碱长花岗岩 279. 2±3. 3Ma 和 278. 2±1. 7Ma,结合地球化学和 Hf 同位素研究,表明古亚洲洋在中二叠世早期尚未闭合(李英雷等,2021)。索伦山蛇绿岩带硅质岩中发现早二叠世放射虫动物群,表明古亚洲洋俯冲消减闭合应在早二叠世后(李钢柱等,2017)。1∶1000000 地质编图和野外地质调查成果表明大兴安岭地区到中—晚二叠世,古亚洲洋盆持续俯冲(杨晓平等,2022)。大兴安岭海西期花岗岩类研究表明,晚泥盆世—中二叠世区域广发发育弧岩浆岩,晚二叠世—早三叠世,古亚洲洋闭合(刘锐等,2016)。九井子蛇绿岩中辉绿岩脉锆石 U-Pb 年龄为 274. 7±1. 7Ma,与蛇绿岩带呈断层接触的粉砂岩碎屑锆石年龄最小值为 249±4. 7Ma,研究表明,索伦—西拉木伦蛇绿岩带闭合于晚二叠世末—早三叠世初(刘建峰等,2016)。色尔崩岩体和努和亭沙拉岩体锆石 U-Pb 年龄为 255. 3±1. 4Ma、254. 4±3. 4Ma,具高锶低钇(adakitic)特征,形成于晚二叠世俯冲背景下(范玉须等,2019)。古地磁数据表明,西伯利亚和华北板块闭合于二叠纪末期(~250Ma)(李朋武等,2006)。林西地区晚二叠世晚期生物礁和海象化石的发现和马达屯期大规模火山喷发以及巴林右旗和吉林九台县的 P/T 角度不整合表明,古亚洲洋在该区域晚二叠世末期闭合(田树刚等,2016)。

研究表明伸展背景包括大陆裂谷带、大陆减薄区、碰撞后伸展环境、与俯冲有关的洋内岛弧、活动陆缘和弧后盆地等多种环境(Hochstaedter et al. ,1990;王焰等,2000)。晚石炭世古亚洲洋俯冲背景下,贺根山区域晚石炭—早二叠发育洋内弧,阿德拉嘎地区处于弧后环境,结合 A 型花岗岩特征,综合分析认为,阿德拉嘎碱长花岗岩形成于弧后伸展构造背景。

5　结论

(1)锆石 LA-ICP-MS U-Pb 测年表明,阿德拉嘎碱长花岗岩的侵位年龄为 310. 7±2. 6Ma,形成时代为晚石炭世。

(2)阿德拉嘎碱长花岗岩具有较高的 SiO2、Na2O+K2O 含量和较高的 Ga/Al、(Na2O+K2O)/CaO 比值,相对贫 CaO、MgO、Sr、Ba、Eu、Ti、P,稀土元素总量较低,轻重稀土分馏不明显,稀土配分曲线呈海鸥型,负铕异常明显(δEu=0. 15~0. 37),为 A 型花岗岩。

(3)岩石学和岩石地球化学特征表明,阿德拉嘎碱长花岗岩为 A 型花岗岩,可能形成于弧后伸展构造环境,为晚石炭世古亚洲洋向西伯利亚板块俯冲作用的产物。

致谢:研究工作得到了中国地质科学院地球深

部探测中心张垚垚博士的指导和帮助；锆石数据得到中国地质科学院矿产资源研究所侯可军博士帮助；审稿专家对论文提出了许多宝贵的意见和建议；在此一并致以衷心的感谢！

注 释 / Notes

❶ 河北省区域地质矿产调查研究所. 2016. 内蒙古 1∶5 万翁根温多尔(L50E017002)、布敦(L50E018001)、柴达木(L50E018002)、必鲁特(L49E019024)、哈达特(L50E019001)、阿德拉嘎乌拉(L50E019002)、阿拉特套高大队(L50E020001)、青克勒宝力格公社幅(L50E020002)区域地质矿产调查

参 考 文 献 / References

(The literature whose publishing year followed by a "&" is in Chinese with English abstract; The literature whose publishing year followed by a "#" is in Chinese without English abstract)

程杨,肖庆辉,李廷栋,郭灵俊,李岩,范玉须,庞进力. 2019. 中亚造山带东缘迪彦庙俯冲增生杂岩带早二叠世洋内弧岩浆作用及构造背景. 地球科学,44(10):3454~3468.

程杨,肖庆辉,李廷栋,许立权,莫凌超,李岩,范玉须,郭灵俊,庞进力. 2020. 西乌旗迪彦庙—达青地区石炭纪斜长花岗岩的发现及其对古亚洲洋构造演化的指示意义. 地质与勘探,56(2):302~314.

程银行,李艳峰,李敏,张天福,牛文超,腾学建,李影,刘洋,彭丽娜. 2014. 内蒙古东乌旗碱性侵入岩的时代、成因及地质意义. 地质学报,88(11):2086~2096.

迟清华,鄢明才. 2007. 应用地球化学元素丰度数据手册. 北京:地质出版社.

邓晋福,冯艳芳,狄永军,刘翠,肖庆辉,苏尚国,赵国春,孟斐,车如风. 2015. 古亚洲构造域侵入岩时—空演化框架. 地质论评,61(6):1211~1224.

邓胜徽,万传彪,杨建国. 2009. 黑龙江阿城晚二叠世安加拉—华夏混生植物群——兼述古亚洲洋的关闭问题. 中国科学 D 辑:地球科学,39(12):1744~1752.

董培培,李英杰,许展,鞠文信,王金芳,李红阳. 2021. 内蒙古查干拜兴晚石炭世埃达克岩的成因及其洋内俯冲作用的约束. 地质学报,95(12):3676~3690.

范玉须,李廷栋,肖庆辉,程杨,李岩,郭灵俊,罗鹏跃. 2019. 内蒙古西乌珠穆沁旗晚二叠世花岗岩的锆石 U-Pb 年龄、地球化学特征及其构造意义. 地质论评,65(1):248~266.

范玉须,肖庆辉,程杨,李岩,刘勇,郭灵俊,庞进力. 2020. 内蒙古迪彦庙孬来可图侵入岩的年代学、Sr—Nd—Hf 同位素特征及其地质意义. 地球科学,45(7):2379~2392.

葛小月,李献华,陈志刚,李伍平. 2002. 中国东部燕山期高 Sr 低 Y 型中酸性火山岩的地球化学特征及成因:对中国东部地壳厚度的制约. 科学通报,47(6):474~480.

洪大卫,王式洸,黄怀增. 1991. 中国北部边疆古生代—三叠纪碱性花岗岩带及其地球动力学意义//李云彤主编. 中国北方花岗岩及其成矿作用论文集. 北京:地质出版社,40~48.

洪大卫,王式洸,谢锡林,张季生. 2000. 兴蒙造山带正 εNd(t)值花岗岩的成因和大陆地壳生长. 地学前缘,7(2):441~456.

侯可军,李延河,田有荣. 2009. LA-MC-ICP-MS 锆石微区原位 U-Pb 定年技术. 矿床地质,28(4):481~492.

贾孝新,童英,游国庆,郭磊. 2017. 内蒙古中部白音乌拉北 A 型花岗岩矿物学、年代学、地球化学及构造意义. 矿物岩石, 37(4):4~16.

金松,李英杰,钱程,张杨,孟都,杨海波,王博,伍光锋. 2022. 内蒙古科右中旗两类基性岩的年代学、地球化学及其构造意义. 地球科学,47(1):342~356.

焦天佳. 2015. 内蒙古苏尼特左旗地区古生代花岗岩岩石学特征. 导师:高永丰. 石家庄,石家庄经济学院硕士学位论文.

李钢柱,王玉净,李成元,白宇明,薛建平,赵广明,薄海军,梁月升,刘伟. 2017. 内蒙古索伦山蛇绿岩带早二叠世放射虫动物群的发现及其地质意义. 科学通报,62(5):400~406.

李锦轶,高立明,孙桂华,李亚萍,王彦斌. 2007. 内蒙古东部双井子中三叠世同碰撞壳源花岗岩的确定及其对西伯利亚和中朝古板块碰撞时限的约束. 岩石学报,23(3):565~582.

李锦轶,刘建峰,曲军峰,郑荣国,赵硕,张进,孙立新,李永飞,杨晓平,王励嘉,张晓卫. 2019a. 中国东北地区主要地质特征和地壳构造格架. 岩石学报,35(10):2989~3016.

李锦轶,刘建峰,曲军峰,郑荣国,赵硕,张进,王励嘉,张晓卫 2019b. 中国东北地区古生代构造单元:地块还是造山带? 地球科学,44(10):3157~3177.

李朋武,高悦,管烨,李秋生. 2006. 内蒙古中部索伦林西缝合带闭合时代的古地磁分析. 吉林大学学报(地球科学版), 36(5):744~758.

李英杰,王金芳,王根厚,李红阳,董培培. 2018. 内蒙古迪彦庙蛇绿岩带达哈特前弧玄武岩的发现及其地质意义. 岩石学报,34(2):469~482.

李英雷,武广,贺宏云,陈公正,杨飞,李铁刚,宋广超,肖剑伟 2021. 内蒙古沙巴尔吐地区中二叠世蛇绿构造混杂岩及同期花岗质杂岩的发现及地质意义. 岩石矿物学杂志,40(2):217~235.

梁日暄. 1994. 内蒙古中段蛇绿岩特征及地质意义. 中国区域地质,(1):36~55.

刘建峰. 2009. 内蒙古林西—东乌旗地区晚古生代岩浆作用及其对区域构造演化的制约[D]. 长春:吉林大学.

刘建峰,李锦轶,孙立新,殷东方,郑培玺. 2016. 内蒙古巴林左旗九井子蛇绿岩锆石 U-Pb 定年:对西拉木伦河缝合带形成演化的约束. 中国地质,43(6):1947~1962.

刘锐,杨振,徐启东,张晓军,姚春亮. 2016. 大兴安岭南段海西期花岗岩类锆石 U-Pb 年龄、元素和 Sr—Nd—Pb 同位素地球化学:岩石成因及构造意义. 岩石学报,32(5):1505~1528.

吕洪波,冯雪东,王俊,朱晓青,董晓朋,张海春,章雨旭. 2018. 狼山发现蛇绿混杂岩——华北克拉通与中亚造山带碰撞边界的关键证据. 地质论评,64(4):777~805.

施光海,苗来成,张福勤,简平,范蔚茗,刘敦一. 2004. 内蒙古锡林浩特 A 型花岗岩的时代及区域构造意义. 科学通报,49(04):384~389.

石文杰,赵旭,魏俊浩,李欢,周红智. 2019. 兴蒙造山带南段白音图嘎地区 A 型花岗岩地球化学特征及其对古亚洲洋演化的制约. 大地构造与成矿学,174(44):141~156.

田树刚,李子舜,张永生,宫月萱,翟大兴,王猛. 2016. 内蒙东部及邻区晚石炭世—二叠纪构造古地理环境及演变. 地质学报,90(4):688~707.

王金芳,李英杰,李红阳,董培培. 2017. 内蒙古梅劳特乌拉蛇绿岩中埃达克岩的发现及其演化模式. 地质学报,91(8),1776~1795.

王金芳,李英杰,李红阳,董培培. 2019. 贺根山缝合带白音呼舒奥长花岗岩锆石 U-Pb 年龄、地球化学特征及构造意义. 地质论评,65(4):857~872.

王金芳,李英杰,李红阳,董培培. 2020. 古亚洲洋晚石炭世俯冲作用:梅劳特乌拉蛇绿岩中扎嘎音高镁安山岩证据. 地质论评,66(2).289~306.

王金芳,李英杰,李红阳,董培培. 2021. 贺根山缝合带晚石炭世 TTG 岩浆事件:奥长花岗岩锆石 U-Pb 年龄和地球化学制约. 地质学报,95(2):396~412.

王树庆,胡晓佳,杨泽黎,刘永顺,刘洋,王文龙,郭硕,何鹏,滕飞. 2020. 1∶500000 二连—东乌旗成矿带西乌旗和白乃庙地区地质图空间数据库. 中国地质,47(S1):21~47.

王树庆,胡晓佳,杨泽黎,赵华雷,张永,郝爽,何丽. 2018. 兴蒙造山带中段锡林浩特跃进地区石炭纪岛弧型侵入岩:年代学、地球化学、Sr—Nd—Hf 同位素特征及其地质意义. 地球科学,43(3):672~695.

王焰,钱青,刘良,张旗. 2000. 不同构造环境中双峰式火山岩的主要特征. 岩石学报,16(2):169~173.

王玉净,樊志勇. 1997. 内蒙古西拉木伦河北部蛇绿岩带中二叠纪放射虫的发现及其地质意义. 古生物学报,36(1):58~68.

肖中军. 2015. 内蒙阿尔善布拉格一带早二叠世碱性花岗岩地球化学特征、锆石 U-Pb 年龄及其地质意义. 地质调查与研究,38(3):171~182.

杨晓平,钟辉,杨雅军,江斌,钱程,马永非,张超. 2022. 大兴安岭地区古生代构造格架重建:来自俯冲增生杂岩研究进展. 地学前缘,29(2):94~114.

张磊,吕新彪,刘阁,陈俊,陈超,高奇,刘洪. 2013. 兴蒙造山带东段大陆弧后 A 型花岗岩特征与成因. 中国地质,40(3):869~884.

张夏炜,程银行,李英杰,许旭,滕学建,王少轶,李影,刘海东. 2021. 内蒙古东乌旗晚石炭世角闪石岩锆石 U-Pb 年龄、地球化学及其构造意义. 地质学报,95(5):1495~1507.

张晓飞,滕超,周毅,王必任,曹军,李树才,张华川,庞振山,刘俊来. 2019. 内蒙古西乌旗地区晚二叠世—早中三叠世花岗岩年代学和地球化学特征及构造意义. 地质学报, 93(8):1903~1927.

张晓飞,周毅,曹军,滕超,王必任,张华川,冯俊岭,刘俊来 2018a. 内蒙古西乌旗罕乌拉地区双峰式侵入体年代学、地球化学特征及其对古亚洲洋闭合时限的制约. 地质学报,92(4):665~686.

张晓飞,周毅,刘俊来,李树才,王必任,滕超,曹军,张华川. 2018b. 内蒙古西乌旗大石寨组火山岩年代学和地球化学特征及地质意义. 岩石学报,34(6):1775~1791.

张玉清,许立全,康小龙,宝音乌力吉. 2009. 内蒙古东乌珠穆沁旗京斯台碱性花岗岩年龄及意义. 中国地质,36(9):988~995.

Belousova E A, Griffin W L, O' Reilly S Y, Fisher N. 2002. Igneous zircon: Trace element composition as an indicator of source rock type. Contributions to Mineralogy and Petrology, 143 (5): 602~622.

Bonin B. 1990. From orogenic to anorogenic setting: Evolution of granitiod suites after a major orogenesis. Geological Journal, 25: 261~270.

Bonin B. 2007. A-type granites and related rocks: Evolution of a concept problems and prospects. Lithos, 97: 1~29.

Cheng Yang, Xiao Qinghui, Li Tingdong, Guo Lingjun, Li Yan, Fan Yuxu, Pang Jinli. 2019&. Magmatism and tectonic background of early Permian intra-oceanic arc in Diyanmiao subduction accretion complex belt in eastern margin of Central Asian Orogenic Belt. Earth Science, 44(10): 3454~3468.

Cheng Yang, Xiao Qinghui, Li Tingdong, Xu Liquan, Mo Lingchao, Li Yan, Fan Yuxu, Guo Lingjun, Pang Jinli. 2020&. Discovery of the Carboniferous plagiogranite in the Diyanmiao—Daqing area of West Ujimqin, Inner Mongolia and its implication to the tectonic evolution of the Paleo-Asian Ocean. Geology and Exploration, 56(2): 302~314.

Cheng Yinhang, Li Yanfeng, Li Min, Zhang Tianfu, Niu Wenchao, Teng Xuejian, Li Ying, Liu Yang, Peng Lina. 2014&. Geochronology and petrogenesis of the alkaline pluton in Dong Ujimqi, Inner Mongolia and tis tectonic implications. Acta Geological Sinica, 88911):2086~2096.

Chi Qinghua, Yan Mingcai. 2007#. Handbook of Elemental abundance for applied geochemistry. Beijing, Geol. Pub. House.

Collins W J, Beams S D, White A J R, Chappell B W. 1982. Nature and origin of A-type granites with particular reference to southeastern Australia. Contributions to Mineralogy and Petrollogy, 80: 189~200.

Cleasson S, Vetrin V, Bayanova T, Downes H. 2000. U-Pb zircon ages from a Devonian carbonatite dyke, Kolapeninsula, Russia: a record of geological evolution from the Archaean to the Palaeozoic. Lithos, 51: 95~108.

Deng Jinfu, Feng Yanfang, Di Yongjun, Liu Cui, Xiao Qinghui, Su Shangguo, Zhao Guochun, Meng Fei, Che Rufeng. 2015&. The intrusive spatial—temporal evolutional framework in the Paleo-Asian tectonic domain. Geological Review, 61(6): 1211~1224.

Deng Shenghui, Wan Chuanbiao, Yang Jianguo. 2009&. Discovery of a Late Permian Angara—Cathaysia mixed flora form Acheng of Heilongjiang, China, with discussions on the closure of the Oaleoasian Ocean. Science inChina(Series D), 39(12): 1744~1752.

Dobretsov N L, BerzinN ;A, Buslov M M. 1995. Opening and tectonic evolution of the Paleo-Asian ocean, Intern, Geol. Rev., 37, 335~360.

Dong Peipei, Li Yingjie, Xu Zhan, Ju Wenxin, Wang Jinfang, Li Hongyang. 2021&. Petrogenesis of the Late Carboniferous adakite in Chaganbaixing, Inner Mongolia and constraints of intra-oceanic subduction, Acta Geologica Sinica, 95(12): 3676~3690.

Eby G N. 1990. The A-type granitoids: A review of their occurrence and chemical characteristics and speculations on their petrogenesis. Lithos, 26: 115~134.

Eby G N. 1992. Chemical subdivision of the A-type granitoids. Petrogenetic and tectonic implications. Geology, 20: 641~644.

Fan Yuxu, Li Tingdong, Xiao Qinghui, Cheng Yang, Li Yan, Guo Lingjun, Luo Pengyue. 2019&. Zircon U-Pb ages, geochemical characteristics of late Permian granite in west Ujimqin Banner, Inner Mongolia, and tectonic significance. Geological Review, 65(1): 248~266.

Fan Yuxu, Xiao Qinghui, Cheng Yang, Li Yan, Liu Yong, Guo Lingjun, Pang Jinli. 2020&. Chronolog, Sr—Nd—Hf isotope geochemistry and geology significance of pluton in the Naolaiketu of Diyanmiao, Inner Mongolia. Earth Science, 45(7) 2379~2392.

Ge Xiaoyue, Li Xianhua, Chen Zhigang, Li Wuping. 2002&. Geochemistry and petrogenesis of Jurassic high Sr/low Y granitoids in eastern China: contrains of crustal thickness. Chinese Science Bulletin, 47(6): 474~480.

Griffin W L, Belousova E A, Shee S R. 2004. Crustal Evolution in the northern Yilarn Craton: U-Pb and Hf-isotope evidence from detrital zircons. Precambrian Research, 131(3~4): 213~282.

Hebei Institute of Regional Geology and Mineral Resuorces. 2016#. 1∶50000 Wenggenwenduo(L50E017002), Budun(L50E018001), Chaidamu (L50E018002), Bilute (L49E19024), Hadate (L50E019001), Adelagawula(L50E019002), Alatetaogaodadui (L50E02001), Qingkelebaoligegongshe (L50E020002) regional geological and mineral survey.

Hochstaedter A G, Gill J B, Kusakabe M, Newman S, Pringle M, Tayor B, Fryer P. 1990. Volcanism in the Sumisu Rift, I. Major

element, volatile, and stable isotope geochemistry. Earth and Planetary Science Letters, 100(1~3): 179~194.

Hollocher, Bull J, Robinson P. 2002. Geochemistry of the metamorphosed Ordovican Taconian Magmatic Arc, Bronson Hill anticlinorium, western New England. Physics and Chemistry of the Earth, 27: 5~45.

Hong Dawei, Wang Shiguang, Huang Huaizeng. 1991&. Preliminary study of the late Paleozoic—Triassic alkaline granite belt in northern territory of China and adiacent area and its geodynamic significance//Li Zhitong. Contributions on granitoids and their Minerogenesis in Northern China. Beijing: Geological Publishing House: 40~48.

Hong DaWei, Wang Shiguang, Xie Xilin, Zhang Jisheng. 2000&. Gensis of positive $\varepsilon_{Nd}(t)$ granitoids in the Da Hing Gan Mts.——Mongolia orogenic belt and growth continental crust. Earth Science Frontiers, 7(2): 441~456.

Hoskin P W O, Black L P. 2000. Metarnorphic zircon formation by solid-state recrystallization of protolith igneous zircon. Journal of Metamorphic Geology, 18: 423~439.

Hoskin P W O, Schaltegger U. 2003. The composition of zircon and igneous and metamorphic petrogenesis. Reviews of Mineralogy and Geochemistry, 53(1): 27~62.

Hou Kejun, Li Yanhe, Tian Yourong. 2009&. In situ U-Pb zircon dating using laser ablation—multi ion counting——ICP-MS. Mineral Deposits, 28(4): 481~492.

Irvine T N, Baragar W R A. 1971. A guide to the chemical classification of the common volcanic rocks. Canad Earth Sci, 8;523~548.

Jia Xiaoxin, Tong Ying, You Guoqing, Guo Lei. 2017&. Mineralogy, geochronology and geochemistry of the Baiyinwulabei A-type granite in the central Inner Mongolia and its tectonic significance. J Mineral Petrol, 37(4): 4~16.

Jian P, Liu D Y, Kroner A, Windley B F, Shi Y R, Zhang F Q, Shi G H, Miao L C, Zhang W, Zhang Q, Zhang L Q, Ren J S, 2008. Time scale of an early to mid-Plaeozoic orogenic cycle of the long-lived Central Asian Orogenic Belt, Inner Mongolia of China: Implications for continental qrowth: Lithos, 101(3~4): 233~259.

Jiao Tianjia. 2015&. The petrology characteristics of the Paleozoic granite in Sonidzuoqi area of Inner Mongolia. Supervisor: Gao Yongfeng. Shijiazhuang, Master thesis of Shijiazhuang University of Economics.

Jin Song, Li Yingjie, Qian Cheng, Zhang Yang, Meng Du, Yang Haibo, Wang Bo, Wu Guangfeng. 2022&. Geichronology and geochemistry of two types of basic rocks in Horqin Right Middle Banner, Inner Mongolia and their tectonic significances. Earth Science, 47(1): 342~356.

King P L, White A J R, Chappell B W. 1997. Characterization and origin of a luminous A type granites of the Lachlan Fold Belt, southestern Australia. J Petrol, 36: 371~391.

Li Jinyi. 2006. Permian geodynamic setting of Northeast China and adjacent regions: closure of the Paleo-Asian Ocean and subduction of the Paleo-Pacific Plate. Journal of Asian Earth Sciences, 26(3~4): 206~324.

Li Gangzhu, Wang Yujing, Li Chengyuan, Bai Yuming, Xue Jianping, Zhao Guangming, Bo Haijun, Liang Yuesheng, Liu Wei. 2017#. Discovery of early Permian radiolarian fauna in the Solon Obo ophiolite belt, Inner Mongolia and its geological significance. Chin Sci Bull, 62(5): 400~406.

Li Jinyi, Gao Liming, Sun Guihua, Li Yaping, Wang Yanbin. 2007&. Shuangjingzi middle Trtassic syn-collisional crust-derived granite in the east Inner Mongolia and its constraint on the timing of collision between Siberian and Sino—Korean paleo-plates. Acta Petrological Sinica, 23(3): 565~582.

Li Jinyi, Liu Jianfeng, Qu Junfeng, Zheng Rongguo, Zhao Shuo, Zhang Jin, Sun Lixin, Li Yongfei, Yang Xiaoping, Wang Lijia, Zhang Xiaowei. 2019a&. Major geological features and crustal tectonic framework of Northeast China. Acta Petrologica Sinica, 35(10): 2989~3016.

Li Jinyi, Liu Jianfeng, Qu Junfeng, Zheng Rongguo, Zhao Shuo, Zhang Jin, Wang Lijia, Zhang Xiaowei. 2019b&. Paleozoic tectonic units of northeast China: continental blocks or orogenic belts. Earth Science, 44(10): 3157~3177.

Li Pengwu, Gao Rui, Guan Ye, Li Qiusheng. 2006&. Paleomagnetic constraints on the final closure time of Solonker—Linxi suture. Journal of Jilin University(Earth Science Edition), 36(5): 744~758.

Li Yingjie, Wang Jinfang, Wang Genhou, Li Hongyang, Dong Peipei. 2018&. Discovery and significance of the Dahate fore-arc basalts from the Diyanmiao ophiolite in Inner Mongolia. Acta Petrologica Sinica, 34(2):469~482.

Li Yinglei, Wu Guang, He Hongyun, Chen Gongzheng, Yang Fei, Li Tiegang, Song Guangchao, Xiao Jianwei. 2021&. The discovery and tectonic implications of Middle Permian ophiolite mélange and coeval granitic complex in the Shabaetu area, Inner Mongolia. Acta Petrological Et Mineralogica, 40(2):217~235.

Liang Rixuan. 1994&. The features of ophiolites in the gentral sector of Inner Mongolia and its ecological significance. Regional Geology of China, 01: 36~55.

Liu Jianfeng. 2009&. Late Paleozoic magmatism and its constraints on regional tectonic evolution in Linxi—Dongwuqi area, Inner Mongolia. Changchun, Jilin University.

Liu Jianfeng, Li Jinyi, Sun Lixin, Yin Dongfang, Zheng Peixi. 2016&. Zircon U-Pb dating of the Jiujingzi ophiolite in Bairin Left Banner, Inner Mongolia: Constraints on the formation and evolution of the Xar Moron River suture zone. Geolog in China, 43(6): 1947~1962.

Liu Yongsheng, Hu Zhaochu, Gao Shan, Gunther D, Xu Juan, Gao Changgui, Chen Hailong. 2008. In situ analysis of major and trace elements of anhydrous minerals by LA-ICP-MS without applying an internal standard. Chemical Geology, 275: 34~43.

Liu Rui, Yang Zhen, Xu Qidong, Zhang Xiaojun, Yao Chunliang. 2016&. Zircon U-Pb ages, elemental and Sr—Nd—Pb isotopic geochemistry of the Hercynian granitoids from the southern segment of the Da Hinggan Mts: Petrogenesis and tectonic implications. Acta Petrologica Sinica, 32(5): 1505~1528 .

Loiselle M C, Wones D R. 1979. Characteristics and Origin of anorogenic granites. Geological Society America Abstracts with Programs, 11: 468.

Lu Hongbo, Feng Xuedong, Wang Jun, Zhu Xiaoqing, Dong Xiaopeng, Zhang Haichun, Zhang Yuxu. 2018&. Ophiolitic Mélanges Found in Mount Langshan as the Crucial Evidence of Collisional Margin between North China Craton and Central Asian Orogenic Belt. Geological Review, 64(4): 777~805.

Ludwig K. 2012. User's manual for Isoplot version 3. 75~4. 15: a geochronological toolkit of Microsoft, Excel Berkley Geochronological Center Special Publication No. 5 .

Middlemost E A K. 1985. Magmas and Magmatic Rocks. London:

Longman: 1~266.

Middlemost E A K. 1994. Naming materials in the magma/igneous rock system. Earth Science Reviews, 37(3~4): 215~224.

Nozaka T, Liu Y. 2002. Petrology of the Hegenshan ophiolite and its implication for the tectonic evolution of northern China. Chemical Geology, 187: 143~173.

Pearce J A, Harris N B W, Tindle A G. 1984. Trace element discrimination diagrams for thetectonic interpretation of granitic rocks. Journal of Petrology, 25: 956~983.

Peccerillo R, Taylor S R. 1976. Geochemistry of eocene calc-alkaline volcanic rocks from the Kastamonu area, Northern Turkey. Contrib Mineral Petrol, 58: 63~81.

Rubatto D, Gebauer D. 2000. Use of cathodoluminescence for U-Pb zircon dating by IOM Microprobe: Some examples form the western Alps. Cathodoluminescence in Geoscience, Springer-Verlag Berlin Heidelberg, Germany. 373~400.

Sengor A M C, Natal'in B A, Burtman V S. 1993. Evolution of the Altaid tectonic collage and Palaeozoic crustal growth in Euraisa. Nature, 354: 209~307.

Shi Guanghai, Miao Laicheng, Zhang Fuqin, Jian Ping, Fan Weiming, Liu Dunyi. 2004#. The age and its district tectonic implications on the Xilinhaote A-type granites, Inner Mongolia. Chinese Science Bulletin, 49(4): 384~389.

Shi Wenjie, Zhao Xu, Wei Junhao, Li Huan, Zhou Hongzhi. 2019&. Geochemical characteristics of A-type granites in Sothern Xingmeng Orogen and constraints on the evolution of the Paleo-Asian Ocean. Geotectonica et Metallogenia, 174(44): 141~156.

Sisson T W. 1994. Hornblende—melt trace-element partitioning measured by ion microprobe. Chem Geol. 117: 331~344.

Streckeisen A. 1976. To each plutonic rock its proper name. Earth-Science Reviews, 12(1): 1~33.

Sun S S, Mcdonough W F. 1989. Chemical and isotopic systematics of ocean basins: Impications for mantle composition and processes. In: Saunders A D and Norry M J(ed.). Magmatism in Ocean Basins, Geological society of London and Blackwell Scientific Publications. London, 313~345.

Sylvester P J. 1989. Post-collisional alkaline granites. Journal of Geology, 97: 261~280.

Sylvester P J. 1998. Post-collisional strongly peraluminous granites. Lithos, 45(1): 29~ 44.

Tang Kedong. 1990. Tectonic development of Paleozoic foldbelts at the north margin of the Sino—Korean craton. Tectonic, 9(2): 249~260.

Tian Shugang, Li Zishun, Zhang Yongsheng, Gong Yuexuan, Zhai Daxing, Wang Meng. 2016&. Late Carboniferous—Permian tectono-geographical conditions and development in eastern Inner Mengolia and adjacent areas. Acta Geologica Sinica, 90(4): 688~707.

Tong Ying, Jahn B M, Wang Tao, Hong Dawei, Smith E I, Sun Min, Gao Jianfeng, Yang Qidi, Huang Wei. 2015. Permian alkaline granites in the Erenhot—Hegenshan belt, northern Inner Mongolia, China: Model of generation, time of emplacement and regional teceonic significance. Journal of Asian Earth Science, 97(Part B): 320~336.

Wang Jinfang, Li Yingjie, Li Hongyang, Dong Peipei. 2017&. Discovery of early Permian intra-oceanic arc adakite in the Meilaotewula ophiolite, Inner Mongolia and its evolution modle. Acta Geologica Sinica, 91(8): 1776~1795.

Wang Jinfang, Li Yingjie, Li Hongyang, Dong Peipei. 2019&. Zircon U-Pb ages and geochemical characteristics of Baiyinhus trondhjemite in Hegenshan suture zone and their tectonic implications. Geological Review, 65(4): 857~872.

Wang Jinfang, Li Yingjie, Li Hongyang, Dong Peipei. 2020&. Late Carboniferous intraoceanic subduction of the Paleo-Asian Ocean: new evidences from the Zagayin high-Mg andesite in the Meilaotewula SSZ ophiolite. Geological Review, 66(2): 289~306.

Wang Jinfang, Li Yingjie, Li Hongyang, Dong Peipei. 2021&. Late Carboniferous TTG magmatic event in the Hegenshan suture zone: zircon U-Pb geochronology and geochemical constraints from the Huduge trondhjemite. Acta Geological Sinica, 95(2): 396~412.

Wang Shuqing, Hu Xiaojia, Yang Zeli, Liu Yongshun, Liu Yang, Wang Wenlong, Guo Shuo, He Peng, Teng Fei. 2020&. 1 : 50000 Geological map spatial database of the Xiwuqi and Bainaimiao areas in the Erlian—Dongwuqi metallogenic belt. Geology in China. 47(S1): 21~47.

Wang Shuqing, Hu Xiaojia, Yang Zeli, Zhao Hualei, Zhang Yong, Hao Shuang, He Li. 2018&. Geochronology, geochemistry, Sr—Nd—Hf isotopic characteristics and geological significance of Carboniferous Yuejin arc intrusive rocks of Xilinhot, Inner Mongolia. Earth Science, 43(3): 672~695.

Wang Yan, Qian Qing, Liu Liang, Zhang Qi. 2000&. Major geochemical characteristics of bimodal volcanic rocks in different geochemical environments. Acta Petrological Sinica, 16(2): 169~173.

Wang Yujing, Fan Zhiyong. 1997&. Discovery of Permian radiolarians in ophiolite belt on northern side of Xarmoron river, Inner Mogolia and its geological significance. Acta Palaeontologica Sinica, 36: 58~69.

Whalen J B, Currie K L, Chappell B W. 1987. A-type granites: geochemical characteristics, discrimination and petrogenesis. Contrib Mineral Petrol, 95: 407 ~419.

Whalen J B, Jenner G A, Longstaffe F J. 1996. Geochemical and isotopic(O, Nd, Pb and Sr) constraints on A-type granite: Petrogensis based on the Topsails igneous suite, Newfoundland Appalachians. Journal of Petrology, 37: 1463~1489.

XiaoWenjiao, Windley B F, Hao Jie, Zhai Mingguo. 2003. Accretion leading to collision and the Permian Solonker suture, Inner Mongolia, China: Termination of the central Asian orogenic belt. Tectonics, 22(6): 8-1~8-20.

Xiao Zhongjun. 2015&. Geochemical Characteristics, Zircon U-Pb Age of the Early Permian Alkaline Granite and its geological significance in the Aershanbulage, Inner Mongolia. Geological survey and research, 38(3): 171~182.

Yang Xiaoping, Zhong Hui, Yang Yajun, Jiang Bin, Qian Cheng, Ma Yongfei, Zhang Chao. 2022&. Research progress on the subduction—accretion complex: Reconstruction of the tectonic framework of the Great Xing'an Range. Earth Science Frontiers, 29(2): 94~114.

Zhang Lei, Lv, Xinbiao, Liu Ge, Chen Jun, Chen Chao, Gao Qi, Liu Hong. 2013&. Characteristics and genesis of continental back-arc A-type granites in the eastern segment of the Inner Mongolia—Da Hinggan Mountains orogenic belt. Geology in China, 40(3): 869~884.

Zhang Xiaohui, Yuan Lingling, Xue Fuhong, Yan Xin, Mao Qian. 2014. Early Permian A-type granites from central Inner Mongolia, North China: Mongolia, Norht China: magmatic trace of post-

collisional tectonics and oceanic crustal recycling. Gondwana Research, 28(1): 311~327.

Zhang Xiawei, Cheng Yinhang, Li Yingjie, Xu Xu, Teng Xuejian, Wang Shaoyi, Li Ying, Liu Haidong. 2021&. Zircon U-Pb dating and geochemistry of the Late Carboniferous hornblendite in Dong Ujimqi Inner Mongolia and its tectonic significance. Acta Geologic Sinica, 95(5): 1495~1507.

Zhang Xiaofei, Teng Chao, Zhou Yi, Wang Biren, Cao Jun, Li Shucai, Zhang Huachuan, Feng Junling, Liu Junlai. 2019&. Geochronology and geochemistry of the Late Permian to Early—Middle Triassic granites in Xiwu Banner, Inner Mongolia and its tectonic significance. Acta Geologica Sinica, 93(8): 1903~1927.

Zhang Xiaofei, Zou Yi, Cao Jun, Teng Chao, Wang Biren, Zhang Huachuan, Feng Junling, Liu Junlai. 2018a&. Geochronological and geochemical features of bimodal intrusive rocks in the Hanwula area of Xiwu Banner, Inner Mongolia: constraints on closure of the Paleo-Asian Ocean. Acta Geologica Sinica, 92(4): 665~686.

Zhang Xiaofei, Zou Yi, Liu Junlai, Li Shucai, Wang Biren, Teng Chao, Cao Jun, Zhang Huachuan. 2018b&. Geochronology and geochemistry for volcanic rocks of Dashizhai Formation and its geological significance in Xi Ujimqin Banner, Inner Mongolia. Acta Geologica Sinica, 34(6):1775~1791.

Zhang Yuqing, Xu Liquan, Kang Xiaolong, Bao Yinwuliji. 2009&. Age dating of alkali granite in Jinggesitaiarea of Dong Ujimqin Banner, Inner Mongolia, and its significance. Geology in China, 36(9): 988~995.

Zhang Zhicheng, Li Ke, Li Jianfeng, Tang Wenhao, Chen Yan, Luo Zhiwei. 2015. Geochronology and geochemistry of the eastern Erenhot ophiolitic complex: Implications for the tectonic evolution of the Inner Mongolia—Daxinganling Orogenic Belt. Journal of Asian Earth Sciences, 97(Part B): 279~293.

Zhu Mingshuai, Baatar M, Miao Laicheng, Anaad C, Zhang Fochin, Yang Shunhu, Li Yueming. 2014. Zircon ages and geochemical compositons of the Manlay ophiolite and coeval island arc: Implications for the tectonic evolution of South Mongolia, 96: 108~122.

Zircon LA-ICP-MS U-Pb age, geochemical character of Adelaga alkali-feldspar granite, in Abaga Banner, Inner Mongolia, and tectonic significance

ZHAO Zenan, WEI Min, YANG Jiankun, NI Keqing, ZHANG Jianzhen, SHEN Jinqing, LIU Tengfei, GE Bin

Hebei regional geological survey institute, Hebei, Langfang 065000

Objectives: This paper provided petrography, geochemical characteristics, LA-ICP-MS zircon U-Pb age of Adelaga alkali feldspar granite, in Abaga Banner, Inner Mongolia. The formation age, genesis and tectonic significance of granits are discussed.

Methods: Based on the field work, through the microscopic observation, the whole rock chemical analysis, the LA-ICP-MS zircon U-Pb isotopic chronology of granites.

Results: The Zircon LA-ICP-MS U-Pb ages indicates that the Adelaga alkali feldspar granite is 310.7±2.6Ma, and formed in Upper Carboniferous. The granite has the character of Higher content of SiO_2, Na_2O+K_2O, higher ratio of Ga/Al, $(Na_2O+K_2O)/CaO$, and relatively poor CaO, MgO, Sr, Ba, Eu, Ti and P. The total amount of rare earth elements is low, the fractionatio of light and heavy rare elements is not aobious, the distribution curve of rare eatrh is seagull, and the anomaly of negative europium is obvious ($\delta Eu=0.15\sim0.37$). The granite belong to A-type granite.

Conclusions: The Adelaga alkali feldspar granite is A-type granite, and formed in back-arc extensional tectonic setting of Upper Carboniferous, which is the product of Paleo-Asian Oceanic subduction to Siberia.

Keywords: Alkali feldspar granite; A-type granite; Zircon U-Pb ages; Upper Carboniferous; Back-arc extensional environoment; Abag Banner, Inner Mongolia.

Acknowledgements: We sincerely thank reviewers and editors for their critical comments and constructive suggestions, which have greatly improved the quality of this paper. This research is financially supported by the project (1212011220451) of China Geological Survey.

First author: ZHAO Zenan, male, born in 1985, engineer, mainly engaged in regional geological and ore field surveyt research work. Email: zhaozenan1985@126.com

Manuscript received on: 2022-04-13; Accepted on: 2022-10-09; Network published on: 2022-10-20

Doi: 10.16509/j.georeview.2022.10.065 **Edited by**: ZHANG Yuxu